

# Latitudinal dynamics of auroral roar emissions

S. G. Shepherd<sup>1</sup> and J. LaBelle

Department of Physics and Astronomy, Dartmouth College, Hanover, New Hampshire

C. W. Carlson

Space Sciences Laboratory, University of California, Berkeley

G. Rostoker

Department of Physics, University of Alberta, Edmonton, Alberta, Canada

**Abstract.** Auroral roar, a narrowband ( $\delta f/f < 0.1$ ) emission near 2 and 3 times the ionospheric electron gyrofrequency ( $2f_{ce}$  and  $3f_{ce}$ ), is observed with a meridional chain of LF/MF/HF radio receivers located in northern Canada spanning 67° to 79° invariant latitude. Observations of these emissions are compared with the auroral electrojet location inferred from the Canadian Auroral Network for the OPEN Program Unified Study (CANOPUS) magnetometer array. Variations in the intensity of the observed auroral roar emissions and in the invariant latitude of the most intense emissions are correlated with movements of the poleward boundary of the electrojet. For example, substorm onsets, which appear as rapid poleward expansions of this boundary, result in screening of the emissions from the underlying ground stations because of precipitation-induced ionization in the lower ionosphere. In four of the five study days the peak emission intensity is located 0°–9° poleward of the poleward electrojet boundary inferred from the magnetometers. In one case the peak emission intensity is up to 10° equatorward of the poleward electrojet boundary. In all cases, there is a tendency for the latitude of the most intense auroral roar emissions to track the movements of the electrojet location inferred from the magnetometer data. For two examples, the footprint of the Fast Auroral Snapshot (FAST) satellite passes within 3° of one or more of the ground stations, and the satellite detects unstable electron populations in the polewardmost auroral arc, reinforcing the scenario that auroral roar emissions are generated by these electrons in the polewardmost arc and propagate into the polar cap where conditions are often favorable for their detection at ground level.

## 1. Introduction

Auroral roar is a relatively narrowband radio emission of auroral origin observed at frequencies of 2.6–3.0 MHz and 4.0–4.5 MHz [Kellogg *et al.*, 1978; Weatherwax *et al.*, 1993]. The emissions are left-hand polarized with respect to the magnetic field [Shepherd *et al.*, 1997] and are composed of fine structures as narrow as  $\sim < 6$  Hz [LaBelle *et al.*, 1995; Shepherd *et al.*, 1998b]. Recently, using radio receivers at sites extending from 66.5° to 79.9° invariant latitude ( $\Lambda$ ), Hughes and LaBelle [1998] studied the variation of  $2f_{ce}$  and  $3f_{ce}$  auroral roar with latitude. They found that the auroral roar frequency in-

creases with increasing latitude, confirming that auroral roar is associated with electron gyroharmonics and that the auroral roar at 2.6–3.0 MHz originates at  $\sim 275$  km altitude if it is generated at the second gyroharmonic. Surprisingly, the peak occurrence rate of  $2f_{ce}$  emissions was found to be at 75°–76°  $\Lambda$ , near the poleward edge of the statistical auroral zone.

This study motivates a closer examination of auroral roar radio emissions measured with the chain of five radio receivers located at the magnetic observatories along an approximate magnetic meridian in northern Canada (see Table 1 and Figures 8 and 9). Magnetometers located at these sites and many others can be used to infer the locations of auroral currents and in particular the latitudes of the electrojet boundaries. By comparing these boundaries with the observed auroral roar emissions on selected days, the latitude dependence of these emissions can be understood in greater detail than was possible in the statistical approach of Hughes and LaBelle [1998].

<sup>1</sup>Now at Applied Physics Laboratory, Johns Hopkins University, Laurel, Maryland.

Copyright 1999 by the American Geophysical Union.

Paper number 1999JA900203.  
0148-0227/99/1999JA900203\$09.00

For this study, 5 days were selected from nearly 4 years of programmable stepped-frequency receiver (PSFR) data (1995–1998). Auroral roar is detected at all five sites in 3 out of the 5 days and at the four most poleward stations in the other 2 days. On all five selected days the intensity of the auroral emissions, as a function of latitude, may be compared with the locations of auroral currents inferred from the magnetometers. During two of the selected days the footprint of NASA's Fast Auroral Snapshot (FAST) satellite passes within several degrees of one or more ground stations at the same time auroral roar is recorded with PSFRs located at these stations. The FAST electron measurements provide a check of the auroral boundary inferred from the magnetometers and measure characteristics of the electron distribution above the probable source region of the emissions.

## 2. Instrumentation

The Dartmouth College PSFRs are located at the sites listed in Table 1 and shown in Figures 8 and 9. These record 30–5000 kHz spectra 20 hours/day at 2 s time resolution. The antennas are sensitive to the magnetic component of the auroral roar emissions, and the power spectral density is computed assuming the waves propagate at the speed of light. Effort has been made to synchronize the stations with Greenwich mean time and with each other to within 2 s. In case studies this synchronization has been verified using anthropogenic signals detected simultaneously with multiple receivers. The different PSFRs use nearly identical antennas, which are  $\sim 10$  m<sup>2</sup> vertical loops. The orientations of the antennas differ at each site since they are adjusted to null local sources of interference. The orientation of the loops does not greatly affect the sensitivity to auroral roar emissions, which are more circularly rather than linearly polarized [Shepherd *et al.*, 1997].

The gains and offsets of the different PSFRs are designed to be as identical as possible. However, in order to compare signals received at the different sites, calibration signals are injected at the preamplifier of each PSFR once each day. Using two calibration signals, one 20 dB below the other, both the gain and the offset of each PSFR can be determined. The resulting signals can be compared to within an accuracy of  $\sim 3$  dB.

The magnetometer array whose coordinates are listed in Table 1 and which is shown in Figures 8 and 9 is operated by the Canadian Space Agency. These sites are equipped with a three-component ring core magnetometer which provides data at a sampling rate of 5 s. A more detailed description of the capabilities of the instruments at these sites is given by Rostoker *et al.* [1995]. The magnetometers are sensitive to currents in the ionosphere, such as the eastward or westward auroral electrojets. By plotting the  $Z$  component of the magnetic disturbance measured by magnetometers along a rough magnetic meridian, the poleward and equatorward borders, as well as the strength, of the auroral electrojet crossing this meridian can be estimated. An east (west) electrojet current, for example, causes a positive (negative) perturbation in the  $Z$  component of the magnetic field at stations north of the current and negative (positive) perturbations at stations south of the current. Deconvolving the observed magnetic signatures with a model including the electrojet and the associated field-aligned currents, which electrically connect the ionosphere and magnetosphere, reveals that the extrema in the latitudinal profile of the  $Z$  component of the disturbance magnetic field provide a good measure of the boundaries of the electrojet. The strength of the electrojet is estimated from the difference between the measured extrema [Kisabeth, 1972], where an electrojet strength of 1 MA uniformly distributed across 5° of latitude produces a perturbation of  $\sim 700$  nT [Rostoker, 1998]. The poleward edge of the auroral electrojet cal-

**Table 1.** Locations in the Northern Hemisphere With Geomagnetic Instrumentation

ID	Site Location	Geographic		Invariant		UT of 2400 MLT
		Lat (N)	Lon (E)	Lat (N)	Lon (E)	
TA <sup>a,b</sup>	Taloyoak, NWT	69.54	266.45	79.1	328.5	0646
BL <sup>a</sup>	Baker Lake, NWT	64.32	263.97	74.2	327.1	0651
RI <sup>b,c</sup>	Rankin Inlet, NWT	62.82	267.89	73.1	334.5	0626
AR <sup>a,b</sup>	Arviat, NWT	61.11	265.95	71.4	331.6	0636
CH <sup>a,b</sup>	Churchill, Manitoba	58.76	265.92	69.1	332.1	0634
GI <sup>a,b,c</sup>	Gillam, Manitoba	56.38	265.36	66.8	331.6	0636
IL <sup>b</sup>	Island Lake, Manitoba	53.86	265.34	64.4	332.0	0635
PI <sup>b,c</sup>	Pinawa, Manitoba	50.20	263.96	60.7	330.5	0640

International Geomagnetic Reference Field (IGRF) Epoch 1998 magnetic model is used. Abbreviations are as follows: ID, site identification; Lat, latitude; Lon, longitude; NWT, Northwest Territories; and MLT, magnetic local time.

<sup>a</sup> Dartmouth programmable stepped-frequency receiver (PSFR) is present.

<sup>b</sup> CANOPUS magnetometer is present.

<sup>c</sup> CANOPUS meridian scanning photometer (MSP) is present.

culated this way is a proxy for the polar cap boundary. The University of Alberta provides a standard analysis of electrojet boundaries and activity level at a 5 min sample rate. They use the Polar Anglo-American Conjugate Experiment (PACE) invariant coordinate system [Baker and Wing, 1989; Gustafsson *et al.*, 1992], which agrees with the International Geomagnetic Reference Field (IGRF) coordinates to within  $\sim 0.5^\circ$ .

NASA's FAST satellite was launched August 21, 1996, into an  $83^\circ$  inclination elliptical orbit of 350 km by 4175 km with an orbit period of 2.4 hours and a  $1.45^\circ$  per year westward precession of the orbit plane. A  $6^\circ$  wide region of the northern auroral zone is thus overflowed by FAST on four consecutive days every  $\sim 25$  days. The precessional period of the perigee latitude is  $\sim 204$  days giving a wide sampling of auroral zone altitudes during the year. Exploiting multiple particle and field sensors including a set of 16 electrostatic analyzers, FAST measures unobstructed  $360^\circ$  electron pitch angle distributions over an energy range of 4 eV to 30 keV at 17 ms time resolution. The high-resolution spatial and temporal measurements in the low-altitude auroral acceleration region allow the study of small-scale plasma interactions at a level unachieved by previous spacecraft [Carlson *et al.*, 1998].

### 3. Data Presentation

The collocation of the Canadian Auroral Network for the OPEN Program Unified Study (CANOPUS) magnetometers and the Dartmouth PSFRs allows the relationship between auroral currents and auroral roar emissions to be studied continuously. For this study we selected 5 days (3 days in 1995 and one each in 1997 and 1998) during which all five PSFRs were operational, auroral roar was seen at several stations, and the emissions either displayed significant time and latitude variations or occurred during a FAST conjunction. The range in magnetic local time (MLT) that is included in this study for each of the five selected days is shown in Figure 1. To provide a larger-scale context for these se-

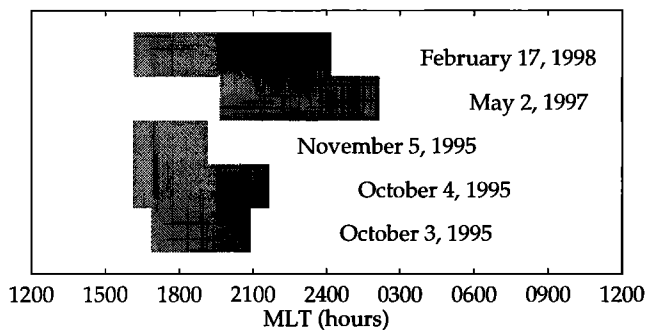


**Figure 1.** The magnetic local time (MLT) range of the auroral roar events studied in this paper, showing the tendency of these events to occur in the pre-midnight sector.

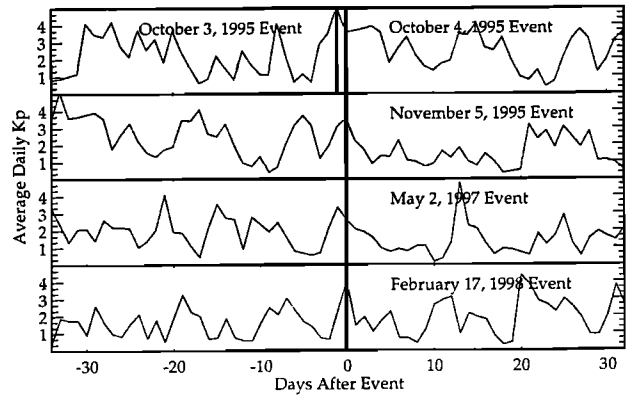


**Figure 2.** The average daily  $K_p$  index for  $\sim 30$  days before and after the events studied in this paper. Vertical lines mark the days chosen for this study.

lected events, the daily average planetary  $K$  indices for 30 days before and after each of the five selected study days are shown in Figure 2.

Figures 3–7 display the PSFR and magnetometer data for each of the five selected days. Figures 3–7 contain grayscale spectrograms of the PSFR data from each of the five sites (Figures 3a–3e, 4a–4e, 5a–5e, 6a–6e, and 7a–7e) and a time series plot of the invariant latitude of the maximum integrated PSFR power (Figures 3f, 4f, 5f, 6f, and 7f). The gray level in the PSFR spectrograms represents the received signal strength, where darker gray pixels represent stronger signals as described in section 2. A given gray level in each plot corresponds to a particular antenna signal level to within  $\sim 3$  dB, as determined from calibration signals described above. The difference in darkness of the background in these plots is due primarily to differences in the background noise level at the stations.

The solid line in Figures 3f, 4f, 5f, 6f, and 7f displays the latitude of the peak emission intensity as measured by integrating the PSFR power over a range of frequencies which includes the auroral roar emission but excludes certain frequencies which are dominated by anthropogenic signals or interference lines. The invariant latitude of each PSFR site is indicated on the right side of Figures 3f, 4f, 5f, 6f, and 7f by the appropriate site abbreviation. The latitude of the peak emission intensity is determined by setting a threshold at the measured power level of the site with the highest or second highest noise level (see discussion below) and discerning the site with the largest emission power above this threshold. Gaps in the line indicate times when no emissions occur above the threshold level, and vertical bars indicate transitions when the peak intensity changes rapidly from one site to another. The coarse spacing of the PSFRs is evident in the large jumps in latitude of this line, but in reality the latitude variations are probably much smoother.

The electrojet boundaries, determined every 5 min from magnetometer data using the method described above, are also shown in Figures 3f, 4f, 5f, 6f, and 7f

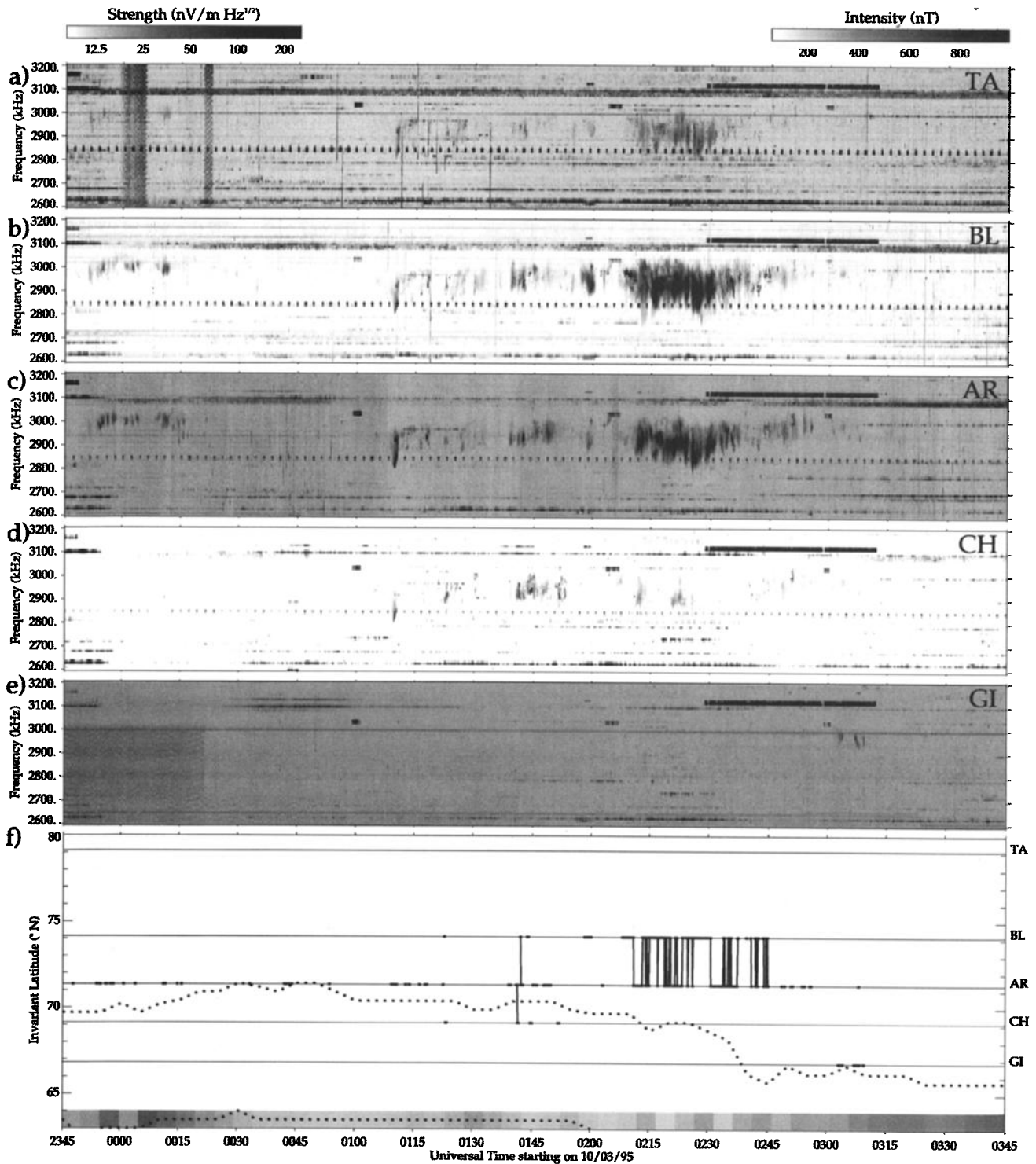


**Figure 3.** Programmable stepped-frequency receiver (PSFR) data at (a) Taloyoak, Northwest Territories, (b) Baker Lake, Northwest Territories, (c) Arviat, Manitoba, (d) Churchill, Manitoba, and (e) Gillam, Manitoba from 2345 UT on October 3, 1995, to 0345 UT on October 4, 1995. (f) The latitude of the peak PSFR intensity and the electrojet boundaries inferred from the CANOPUS magnetometer data for the same period.

as dotted lines. Along the bottom of Figures 3–7 a grayscale strip represents the strength of the electrojet currents with darker gray indicating stronger currents. The two grayscale colorbars above Figures 3a, 4a, 5a, 6a, and 7a indicate the intensity of auroral roar emis-

sions in Figures 3a–3e, 4a–4e, 5a–5e, 6a–6e, and 7a–7e and the strength of the electrojet at the bottom of Figures 3f, 4f, 5f, 6f, and 7f, respectively.

The large variation in the intensity of the background noise detected at the five sites requires that the signals

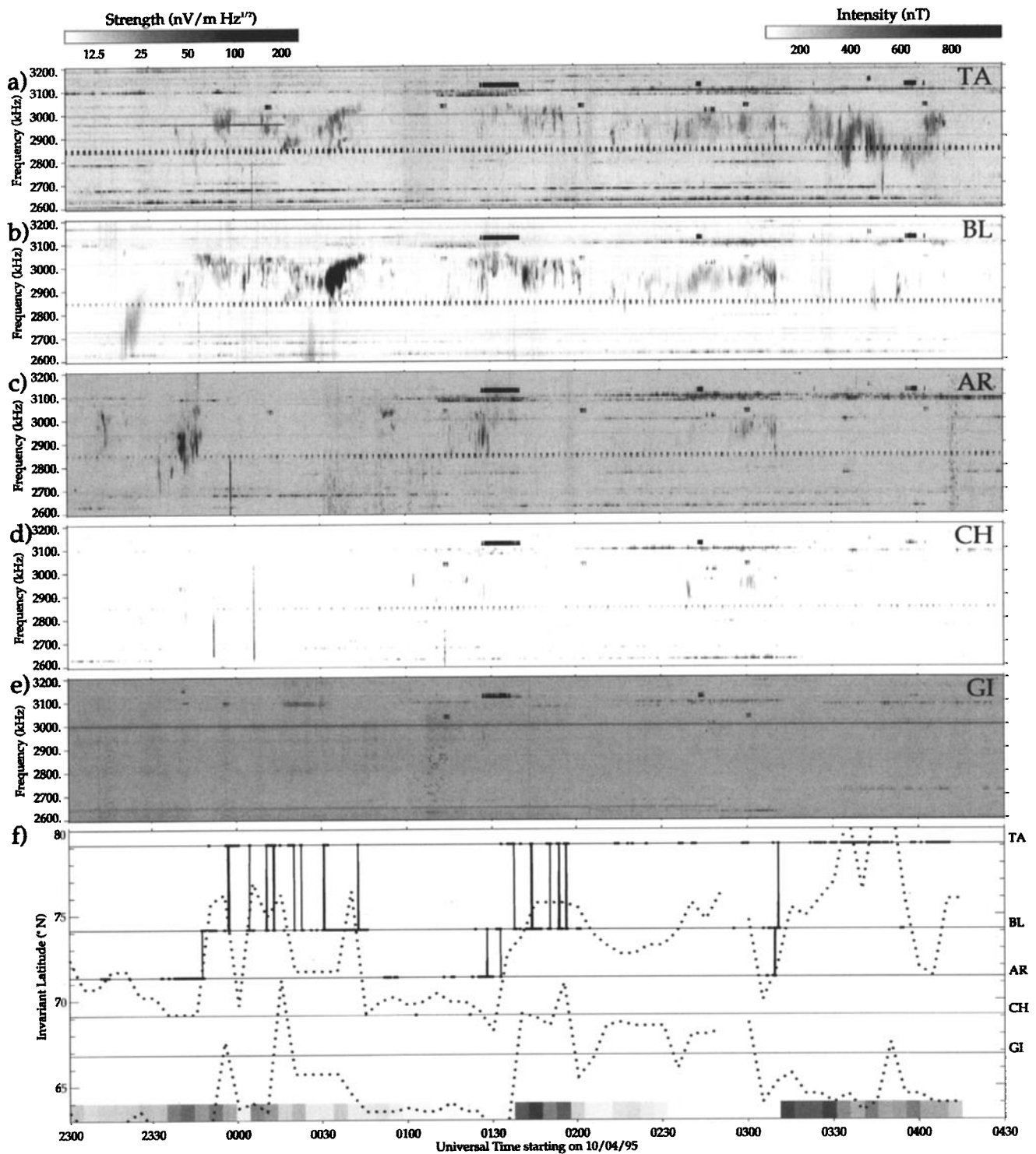


**Figure 4.** Programmable stepped-frequency receiver (PSFR) data at (a) Taloyoak, Northwest Territories, (b) Baker Lake, Northwest Territories, (c) Arviat, Manitoba, (d) Churchill, Manitoba, and (e) Gillam, Manitoba from 2300 UT on October 4, 1995, to 0430 UT on October 5, 1995. (f) The latitude of the peak PSFR intensity and the electrojet boundaries inferred from the CANOPUS magnetometer data for the same period.

be compared carefully in order to assure that the latitude of maximum wave intensity is not determined by the background noise at any station and that the site of maximum wave intensity is not identified in cases where another site, with higher background noise, could rea-

sonably have harbored more intense but undetectable emission signals. For two days, May 2, 1997, and February 17, 1998, the threshold level for determining the latitude of maximum auroral roar emission was set at the background level of the Churchill receiver ( $4.5 \times 10^{-10}$

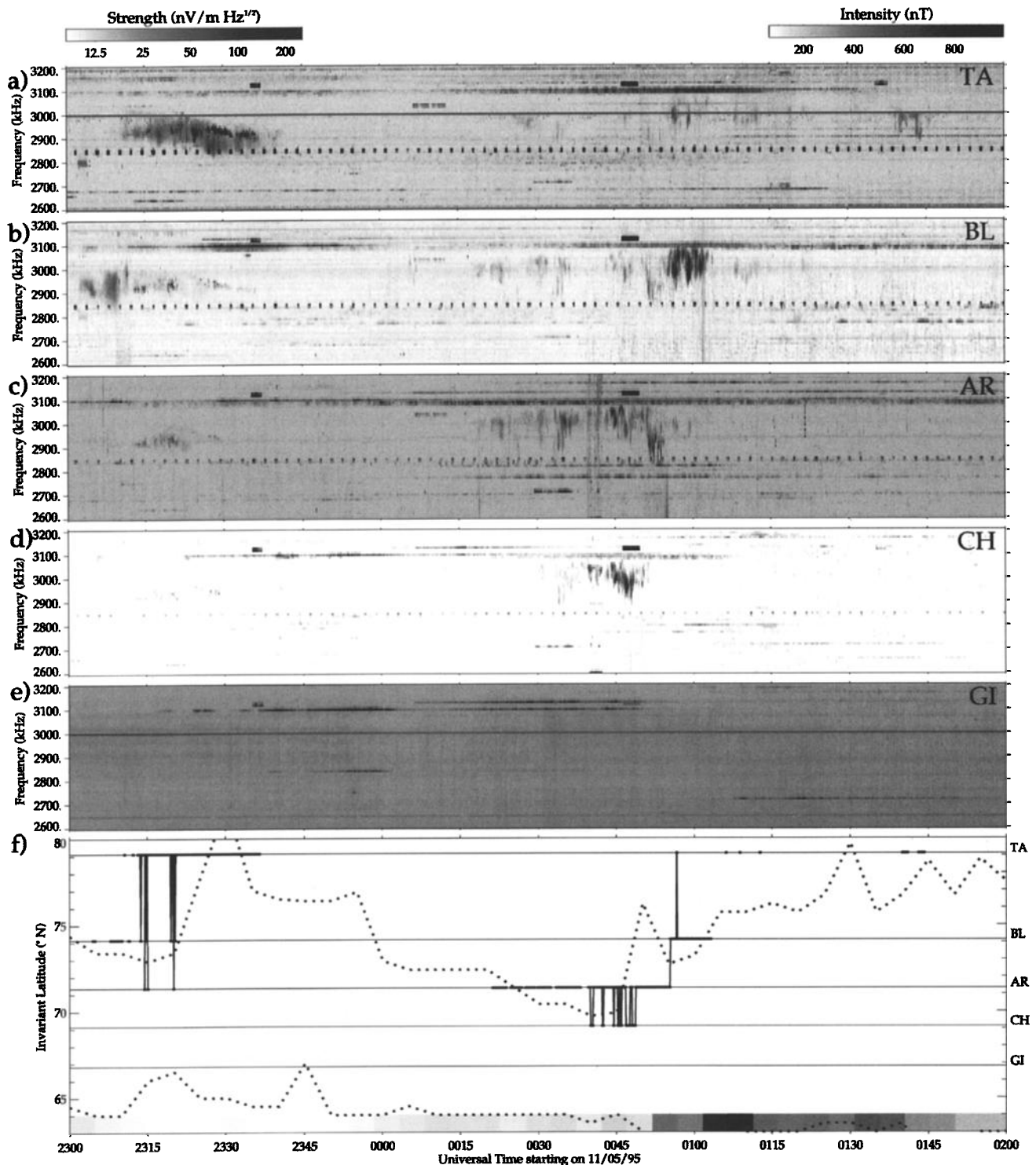


**Figure 5.** Programmable stepped-frequency receiver (PSFR) data at (a) Taloyoak, Northwest Territories, (b) Baker Lake, Northwest Territories, (c) Arviat, Manitoba, (d) Churchill, Manitoba, and (e) Gillam, Manitoba from 2300 UT on November 5, 1995, to 0200 UT on November 6, 1995. (f) The latitude of the peak PSFR intensity and the electrojet boundaries inferred from the CANOPUS magnetometer data for the same period.

$V^2/m^2$ ), which during this time had the least sensitivity because of the installation of a smaller antenna there in 1997–1998 for polarization measurements [see *Shepherd et al.*, 1997]. For the other 3 days the threshold level was set at the background level of the Arviat re-

ceiver ( $2.0 \times 10^{-11} V^2/m^2$ ), in effect ignoring the data from the Gillam receiver at the southern extreme of the chain, which had a significantly higher background noise level, except for a short time during the October 4, 1995, event when the emissions are clearly most in-

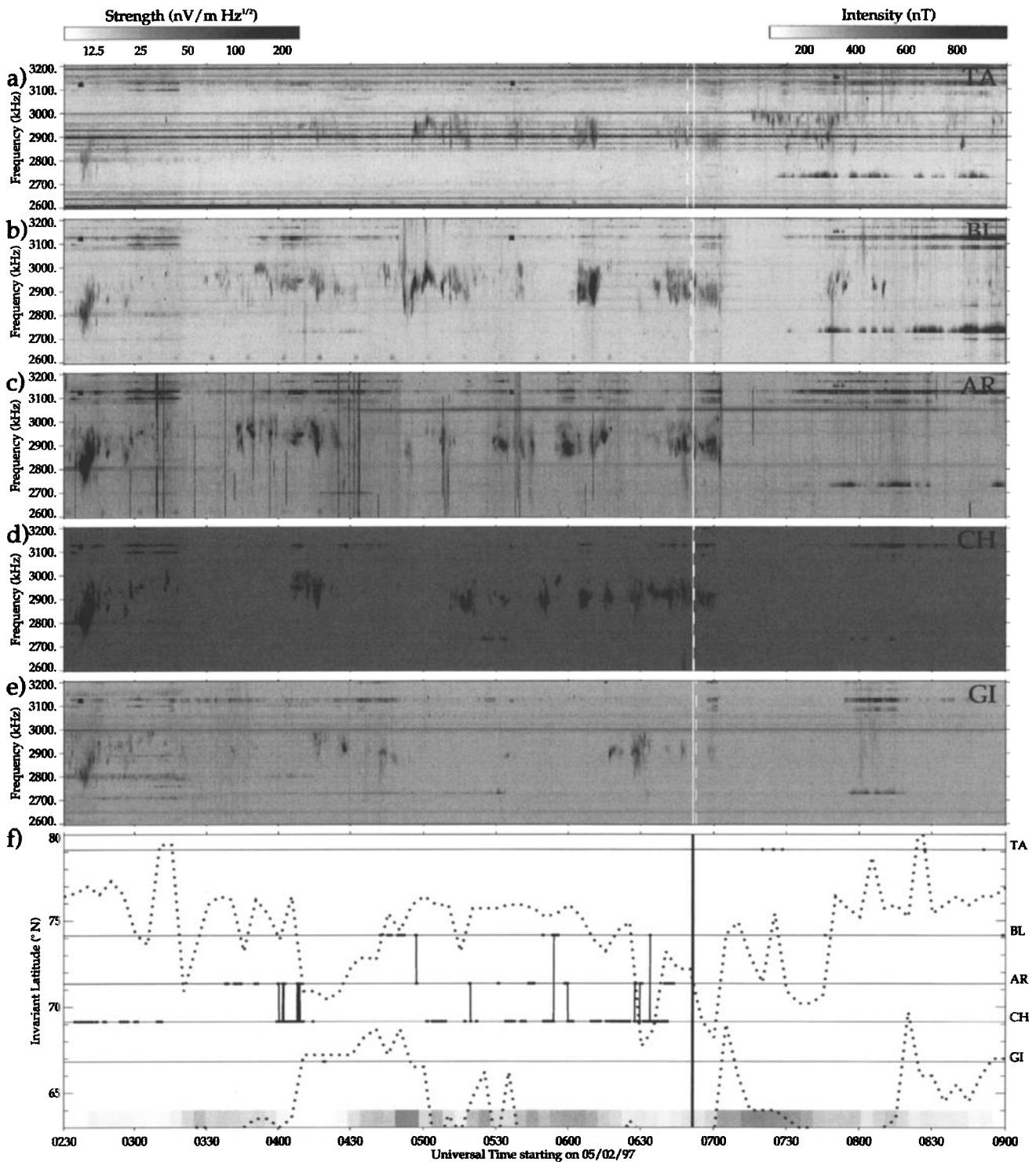


**Figure 6.** Programmable stepped-frequency receiver (PSFR) data at (a) Taloyoak, Northwest Territories, (b) Baker Lake, Northwest Territories, (c) Arviat, Manitoba, (d) Churchill, Manitoba, and (e) Gillam, Manitoba from 0230 to 0900 on May 2, 1997. (f) The latitude of the peak PSFR intensity and the electrojet boundaries inferred from the CANOPUS magnetometer data for the same period. The vertical dashed lines indicate the times of the Fast Auroral Snapshot (FAST) overflight of each station, and the solid vertical line indicates the time FAST passes into the precipitation region (see Figure 10).

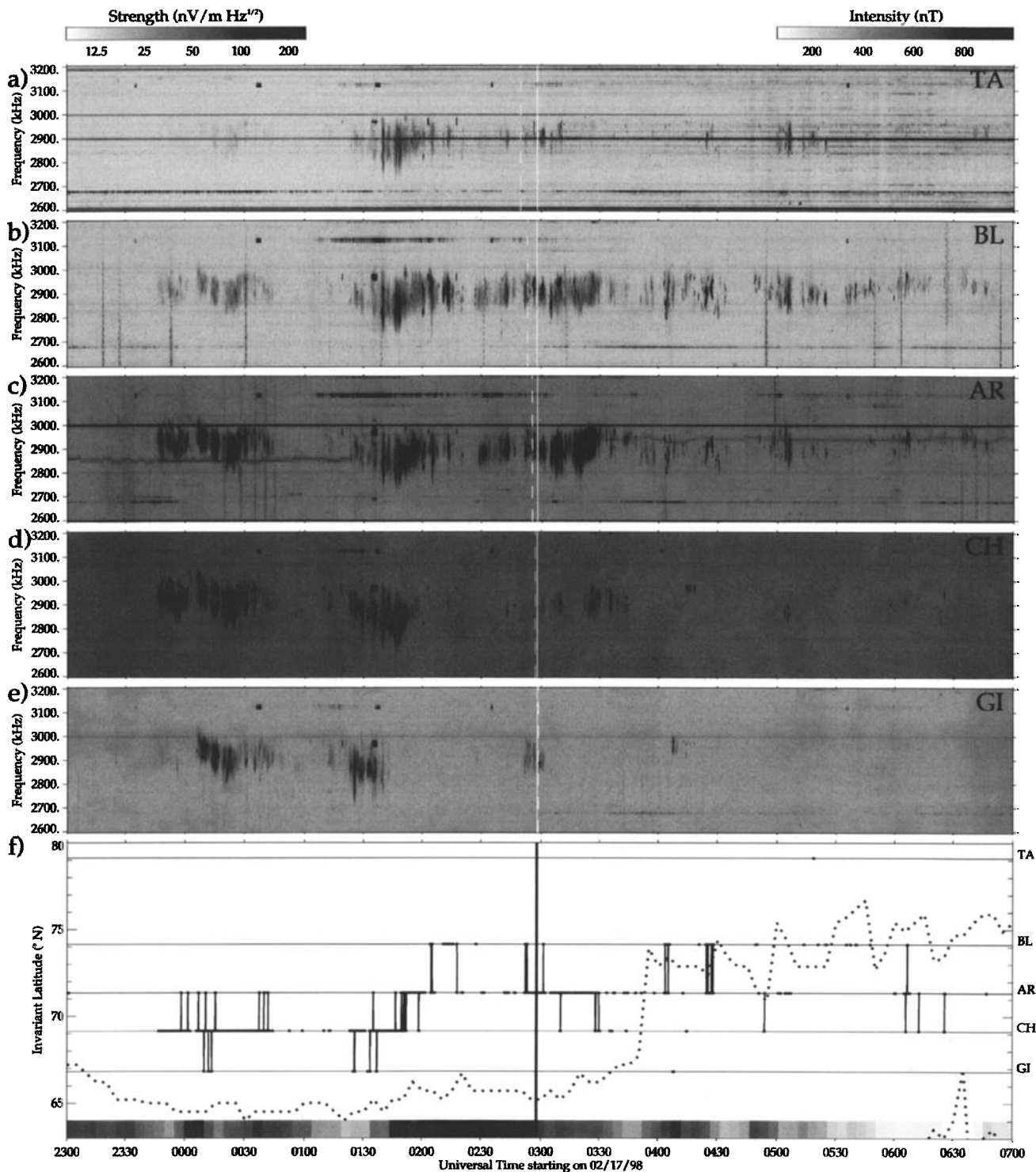


**Figure 7.** Programmable stepped-frequency receiver (PSFR) data at (a) Taloyoak, Northwest Territories, (b) Baker Lake, Northwest Territories, (c) Arviat, Manitoba, (d) Churchill, Manitoba, and (e) Gillam, Manitoba from 2300 UT on February 17, 1998 to 0700 UT on February 18, 1998. (f) The latitude of the peak PSFR intensity and the electrojet boundaries inferred from the CANOPUS magnetometer data for the same period. The vertical dashed lines indicate the times of the FAST overflight of each station, and the solid vertical line indicates the time FAST passes into the precipitation region (see Figure 11).

tense at Gillam. By choosing the lower threshold and ignoring the Gillam data when the auroral roar activity was clearly centered at the poleward stations, a much clearer picture of the latitude variations of the emissions is obtained than would be possible if the only emissions studied were those that exceeded the rather high noise level of the Gillam receiver. In all 5 days some data points for the solid line, representing the latitude of the peak emissions, have been removed to eliminate spurious peaks due to intermittent anthropogenic signals, atmospherics, or other radio noise.

### 3.1. October 3, 1995

Figure 3 displays PSFR and magnetometer data recorded at 2345 UT on October 3 to 0345 UT on October 4, 1995 (1653–2053 MLT). On this day the magnetic perturbations from the electrojet were moderate (100–550 nT), and the poleward boundary was relatively stationary ( $66^{\circ}$ – $71^{\circ}$ ). For reference, the daily average  $Kp$  was 3.5 for October 3 and 5.1 for October 4 (Figure 2).

An auroral roar emission begins at the start of the record, just before midnight UT, and lasts for roughly 30 min. During this half hour the emissions are detected only at stations poleward of  $\sim 70^{\circ}$ , and the highest intensity occurs at Arviat ( $71^{\circ}$ ). The poleward edge of the electrojet determined from the magnetometer data during this period moves slowly poleward from  $69^{\circ}$  to  $71^{\circ}$ . No auroral roar emissions are detected at ground stations equatorward of this poleward electrojet boundary.

The auroral roar emissions cease for nearly 1 hour and then occur again at all stations except for Gillam. From  $\sim 0100$ – $0200$  UT the peak intensity occurs at Arviat ( $71^{\circ}$ ) and occasionally at Churchill ( $69^{\circ}$ ), alternately poleward and occasionally equatorward of the poleward edge of the electrojet, which stays around  $70^{\circ}$ . Beginning at  $\sim 0200$  UT the emissions greatly intensify for nearly 30 min and are strongest between Arviat and Baker Lake ( $72^{\circ}$ – $74^{\circ}$ ) up to  $5^{\circ}$  poleward of the poleward electrojet boundary during this time.

As the roar emissions weaken after 0240 UT, the peak intensity moves equatorward to Arviat, shortly after the poleward edge of the electrojet retreats equatorward of Gillam ( $67^{\circ}$ ), where it remains for the duration of the record. Auroral roar emissions are strongest at Gillam from 0300 to 0310 UT. In fact, the only time during this record when auroral roar is detected at Gillam is during this period when the poleward boundary of the electrojet is at its farthest equatorward position, south of Gillam.

### 3.2. October 4, 1995

Figure 4 displays data recorded 2300 UT on October 4 to 0430 UT on October 5, 1995 (1608–2138 MLT) in the same format as Figure 3. On October 5 the average daily  $Kp$  was 3.6, the electrojet produced magnetic perturbations ranging from  $\sim 60$ – $700$  nT, and the latitude

variations of the auroral currents were more dynamic than on October 3–4.

Auroral roar is first detected exclusively at Arviat ( $71^{\circ}$ ) beginning near 2310 UT when the poleward boundary of the electrojet is also located at  $\sim 71^{\circ}$ . The most intense emissions continue to be recorded at Arviat until 2347 UT. During 2347–2352 UT the latitude of peak emission intensity moves poleward to Baker Lake ( $74^{\circ}$ ) and then to Taloyoak ( $79^{\circ}$ ), with the roar emission disappearing first at Churchill and then at Arviat. The poleward edge of the electrojet follows a similar path, expanding from  $\sim 69^{\circ}$  at 2340 UT to  $\sim 76^{\circ}$  at 2355 UT.

During 0015–0050 UT the poleward edge of the electrojet retreats equatorward. Over the same time the latitude of the most intense emissions shifts from Taloyoak (0015 UT) to Baker Lake (0035 UT) to Arviat (0050 UT). Between 0100 and 0130 UT the poleward edge of the electrojet stays near  $70^{\circ}$ , and what little emissions occur remain concentrated at Arviat ( $71^{\circ}$ ).

From 0130 to 0145 UT the latitude of the peak intensity moves poleward from Arviat to Baker Lake and then to Taloyoak. The electrojet boundary moves from  $68^{\circ}$  to  $76^{\circ}$  during this same period and remains above  $\sim 72^{\circ}$  until 0300 UT. During this time, auroral roar emissions are detected primarily at Baker Lake and Taloyoak with the peak intensity most often at Taloyoak.

After 0305 UT the electrojet boundary shifts poleward, reaching  $>80^{\circ}$  at 0335 UT and 0345–0350 UT. The auroral roar also shift poleward, with the highest intensity recorded at Taloyoak. In fact, auroral roar is detected exclusively at Taloyoak from 0320 to 0410 UT, except for two brief periods near 0345 and 0354 UT when emissions are also detected at Baker Lake. A brief burst of intense emissions is detected at Baker Lake just before  $\sim 0354$  UT, just preceding the equatorward shift in the poleward electrojet boundary at 0355 UT and at about the same time that the equatorial electrojet boundary jumps poleward from  $64^{\circ}$  to  $68^{\circ}$  and back to  $65^{\circ}$ .

Two substorm onsets can be seen during this day, a rather weak one at 0130–0145 UT, the radio frequency effects of which extend only as far north as Arviat ( $71^{\circ}$ ), and a stronger one at 0305–0330 UT, the effects of which extend to Taloyoak ( $79^{\circ}$ ). One signature of a substorm onset in the PSFR data is a brief intensification of auroral roar emissions before an abrupt cutoff. The poleward boundary of the electrojet expands poleward as the electrojet intensity increases during a typical substorm onset.

### 3.3. November 5, 1995

Figure 5 displays PSFR and magnetometer data recorded 2300 UT on November 5 to 0200 UT on November 6, 1995 (1608–1908 MLT), including two periods of dynamic latitude variations in the auroral currents. For reference, the average daily  $Kp$  was 3.1 on November 5

and 3.6 on November 6, and the magnetic perturbations of the electrojet varied from  $\sim 60$  to 1020 nT.

Auroral roar is first detected at Baker Lake ( $74^\circ$ ) near 2300 UT, at which time the poleward boundary of the electrojet is also near  $74^\circ$ . At 2315 UT the latitude of the highest emission intensity shifts from Baker Lake ( $74^\circ$ ) to Taloyoak ( $79^\circ$ ), anticipating the sudden poleward shift in the electrojet boundary at 2320 UT. This sudden poleward shift is indicative of a substorm onset similar to those noted during the October 4 event. However, unlike the two substorm onsets on that day, there is no significant increase in the magnitude of the electrojet currents during this poleward shift. The most intense emissions occur at Taloyoak ( $79^\circ$ ) and remain there until  $\sim 2337$  UT when the emissions completely disappear at all five stations.

Auroral roar is again observed starting at  $\sim 0015$  UT. The latitude of peak intensity is at Arviat ( $71^\circ$ ) during 0015–0040 UT and then shifts equatorward, fluctuating between Arviat and Churchill ( $69^\circ$ – $71^\circ$ ) during 0040–0050 UT. The electrojet boundary is slightly poleward of the peak emissions at 0015 UT and moves gradually equatorward from  $73^\circ$  to  $70^\circ$  during this period, in parallel with the observed equatorward shift of the emissions.

At 0050 UT the poleward electrojet boundary moves rapidly poleward and undulates a bit, reaching  $77^\circ$  at 0105 UT, after which it moves poleward more gradually. The auroral roar intensity mimics this poleward motion, shifting from Churchill ( $69^\circ$ ) at 0047 UT to Arviat ( $71^\circ$ ) at 0047–0055 UT to Baker Lake ( $74^\circ$ ) at 0055–0105 UT to Taloyoak ( $79^\circ$ ) at 0115 UT. The final observations of auroral roar on this day near 0140 UT are most intense at Taloyoak, consistent with the rather extreme poleward location of the electrojet boundary, which even exceeds  $80^\circ$  for short times.

The period from 0045 to 0120 UT is another clear example of a substorm onset like the two examples in the October 4 event. The most intense auroral emissions shift rapidly poleward with the poleward expansion of the electrojet boundary, ceasing at stations equatorward of this boundary, and the intensity of the electrojet increases dramatically from 157 to 1020 nT.

### 3.4. May 2, 1997

Figure 6 displays PSFR and magnetometer data recorded from 0230 to 0900 UT (1939–0209 MLT) on May 2, 1997. On this day the average  $Kp$  was 2.7, and the magnetic perturbations of the electrojet were again moderate, similar to the October 3 event ( $\sim 60$ – $410$  nT). Auroral roar is detected at all five stations for much of this period, and at least two substorms occur. Unlike all of the other 4 days in this study, the latitude of the peak intensity of auroral roar emissions is most often equatorward of the poleward edge of the electrojet boundary, often by up to  $\sim 8^\circ$ . However, as on the other days, the latitude of the most intense emissions tends to roughly track the poleward electrojet boundary.

During 0230–0315 UT, auroral roar is detected at all five stations ( $67^\circ$ – $79^\circ$ ) but the peak intensity is observed at Churchill ( $69^\circ$ ). At this time the auroral zone inferred from the magnetometers covers the latitude range  $\sim 60^\circ$ – $77^\circ$ ; in other words, the strongest auroral roar lies nearly  $8^\circ$  equatorward of the poleward edge of the auroral oval.

A substorm occurs at 0315 UT, and during the recovery phase the latitude of most intense auroral roar decreases from  $71^\circ$  to  $69^\circ$ , in parallel with but equatorward of the poleward electrojet boundary, which shifts from  $77^\circ$  at 0330 UT to  $71^\circ$  at 0415 UT. Briefly, at 0425 UT the auroral roar is most intense at Gillam ( $67^\circ$ ) which is equatorward of the low-latitude electrojet boundary. During 0415–0500 UT the auroral emissions shift poleward from  $69^\circ$  to  $74^\circ$ , again coincident with a similar poleward shift in the poleward electrojet boundary, except that in this interval the poleward electrojet boundary and the latitude of strongest emissions nearly coincide.

From 0500 to 0600 UT the latitude of peak auroral roar intensity alternates between Churchill ( $69^\circ$ ) and Arviat ( $71^\circ$ ), and the poleward electrojet boundary remains far to the north, near  $76^\circ$ . Between 0600 and 0700 UT the peak emissions are concentrated at Churchill, except for a brief time near 0610 UT when the most intense emissions occur at Baker Lake. During this time the poleward electrojet boundary generally shifts equatorward but still lies poleward of the latitude of most intense auroral roar. After the substorm onset at 0700 UT the boundary shifts around but generally moves poleward from  $69^\circ$  at 0700 UT to  $77^\circ$  after 0800 UT. During this time the emissions also shift poleward, occurring at Baker Lake and Taloyoak during the substorm recovery. During this final part of the record (0730–0900 UT) the more usual pattern reasserts itself; that is, the auroral roar occurs at or poleward of the poleward electrojet boundary.

The first substorm during the time period of this event occurs at  $\sim 0315$  UT when the distant propagating natural and anthropogenic signals abruptly cease in all five stations. The electrojet boundary moves rapidly poleward, indicating an expanding auroral oval, and the magnetic perturbations due to the electrojet currents increase moderately from 119 to 275 nT at 0310–0325 UT. During the recovery phase the electrojet boundary generally moves equatorward as the emissions reappear at the northern stations first: Baker Lake ( $\sim 0330$  UT), Arviat ( $\sim 0345$  UT), Churchill ( $\sim 0405$  UT), and finally at Gillam ( $\sim 0420$  UT). The impulsive signals in the Arviat PSFR data are not related to the aurora and are caused by distant atmospheric events.

During the second substorm commencing at 0703 UT, MF-burst emissions are recorded at Arviat, Baker Lake, and Taloyoak just prior to the dramatic loss of signals at all five stations, which is frequently observed during substorm onsets [LaBelle *et al.*, 1994]. The intensity of the electrojet currents experiences a more dramatic

increase than the previous substorm from 138 to 397 nT at 0640–0720 UT. Again, during the recovery phase the signals clearly reappear first at the more northern stations; the gap in emissions at Taloyoak is only a few minutes.

### 3.5. February 17, 1998

Figure 7 displays PSFR and magnetometer data recorded at 2300 UT on February 17 to 0700 UT on February 18, 1998 (1610–0010 MLT). The average daily  $K_p$  index is 2.4 on February 17 and 4.1 on February 18, and the magnetic perturbations due to the electrojet currents range from  $\sim 60$  to 1080 nT.

Auroral roar is detected at all five ground stations beginning near 2330 UT. During 2330–0145 UT the emissions are generally most intense at Churchill (69°). From 0145 to 0330 UT the activity shifts mostly to Arviat (71°) except for short intervals near 0205 and 0215 UT. The poleward electrojet boundary is consistently equatorward of the latitude of the most intense emissions and is relatively constant between 64° and 67° during this period, implying that the emissions are most intense well poleward of the electrojet boundary by up to 7°.

After 0330 UT the latitude of the peak emissions shifts somewhat poleward, fluctuating between Arviat and Baker Lake, except for one brief burst of auroral roar at 0410 UT which is detected strongest at Gillam,  $\sim 6^\circ$  inside of the poleward electrojet boundary. The electrojet boundary also moves poleward from 65° at 0300 UT to 72°–77° at 0400–0700 UT. Auroral roar emissions are detected intermittently at the four northernmost stations during this period, peaking poleward of the electrojet boundary at Taloyoak, near the bound-

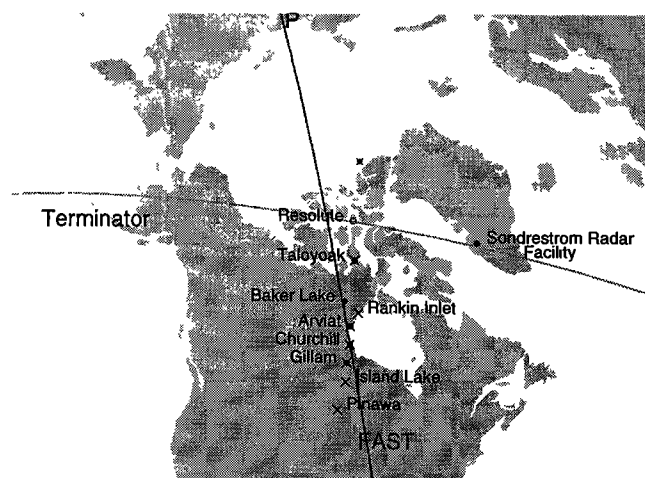


**Figure 8.** The footprint of the FAST satellite during orbit 2745. The geographic location of the Dartmouth College northern hemisphere PSFRs (circles) and the Canadian Auroral Network for the OPEN Program Unified Study (CANOPUS) magnetometers (crosses) are shown for reference. The dawn-dusk terminator is also shown.

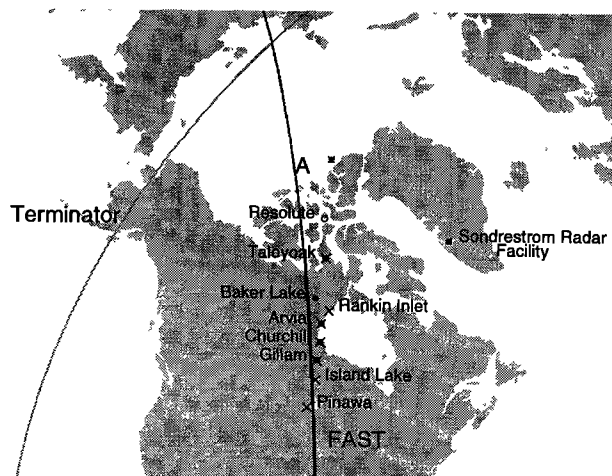


**Figure 9.** The footprint of the FAST satellite during orbit 5903. The geographic location of the Dartmouth College northern hemisphere PSFRs (circles) and the CANOPUS magnetometers (crosses) are shown for reference. The dawn-dusk terminator is also shown.

ary at Baker Lake, and equatorward at Arviat and Churchill.

## 4. FAST Conjunctions

Besides the magnetometer array which provides a continuous but low-spatial resolution monitor of the auroral currents, on occasions satellite overflights provide higher-resolution measurements. Since the launch of the FAST satellite in August 1996, there have been hundreds of orbits where the footprint of FAST (mapped to 100 km) has passed within  $3^\circ$  of one or more of the PSFR ground stations. Eight such conjunctions have been identified during which auroral roar is observed at one or more of these sites. During two of these the PSFRs at all five ground stations were operational: May 2, 1997 and February 17–18, 1998. PSFR data from these two nights are shown in Figures 6 and 7 and discussed above.

The footprint of FAST is computed by mapping the location of the spacecraft down the field line to a point in the Earth's ionosphere (100 km altitude) that is magnetically connected to the satellite location in space. The IGRF model with extrapolated secular variation [*International Association of Geomagnetism and Aeronomy Division I Working Group 1, 1985*] is used for the Earth's magnetic field in this computation. Dark lines in Figures 8 and 9 show the footprint of FAST relative to the ground stations during the two conjunctions on May 2, 1997, and February 17, 1998, respectively. The motion of the satellite is equatorward (down) in both cases. The lighter line in these plots indicates the dawn-dusk terminator. FAST covers the entire latitude range of the PSFRs (67°–79°) within 5–10 min, in effect providing a snapshot of auroral properties along a cut through the oval at the conjunction time.

Figures 10 and 11 display data from the electrostatic analyzers aboard FAST during the two overflights. Figures 10a, 10b, 11a, and 11b show electron energy flux versus energy for the pitch angle ranges  $0^\circ$ – $30^\circ$  and  $150^\circ$ – $180^\circ$ , respectively, where  $0^\circ$  corresponds to earthward (downgoing) and  $180^\circ$  corresponds to anti-earthward (up-going) directions. Figures 10c and 11c show electron energy flux versus pitch angle for energies exceeding 1 keV. No wave data above 2 MHz are available for these orbits.

Figures 10d and 11d represent the power of the auroral roar emissions detected at each of the ground stations during the FAST overpass. The measured power is averaged for a 4 min interval centered on the time when FAST passes over the polar cap boundary, which is inferred from the sudden increase in the measured electron flux at energies capable of producing visible aurorae ( $>0.1$  keV). The solid line indicates the integrated and averaged power at each station, excluding Churchill. Since the noise level at Churchill is  $\sim 10$  dB higher than that for any of the other PSFRs because of the low sensitivity of the polarization antenna, a straight comparison of power is biased by the differing noise levels and therefore is not very insightful. In order to better represent the relative intensity of the observed emissions between sites, the dotted line in Figures 10d and 11d represents the power above the

Churchill noise level ( $\sim 4.0 \times 10^{-10} \text{ V}^2/\text{m}^2$ ), integrated over the frequency range specified and averaged for 4 min around the FAST polar cap boundary crossing. From these two lines the real power at the stations can be envisioned by continuing the solid line to include Churchill using the dotted line as an estimate of the relative intensities. A power level of  $\leq 5 \times 10^{-12} \text{ V}^2/\text{m}^2$  indicates there were no observed emissions above the Churchill noise level. Tick marks at the bottom of Figures 10d and 11d indicate when the footprint latitude of FAST coincides with that of each ground station.

#### 4.1. May 2, 1997

Figure 8 shows the footprint of FAST during its orbit (2745) on May 2, 1997. This orbit was a perigee pass of the Northern Hemisphere, and the altitude of the spacecraft was  $\sim 600$ – $800$  km. The footprint of FAST passes from the polar cap into the auroral zone near several of the PSFR ground stations during the period  $\sim 0648$ – $0652$  UT ( $\sim 2345$ – $0100$  MLT). The vertical dashed lines in Figure 6 indicate when the footprint of FAST is at the same latitude as the ground stations. The solid vertical line marks the time when the footprint of FAST passes the polar cap boundary, indicated in Figures 10a–10c by a dramatic increase in electron energy flux at 0651:00 UT ( $\sim 70^\circ$ ). The agreement of this boundary and the poleward edge of the electrojet inferred from magne-

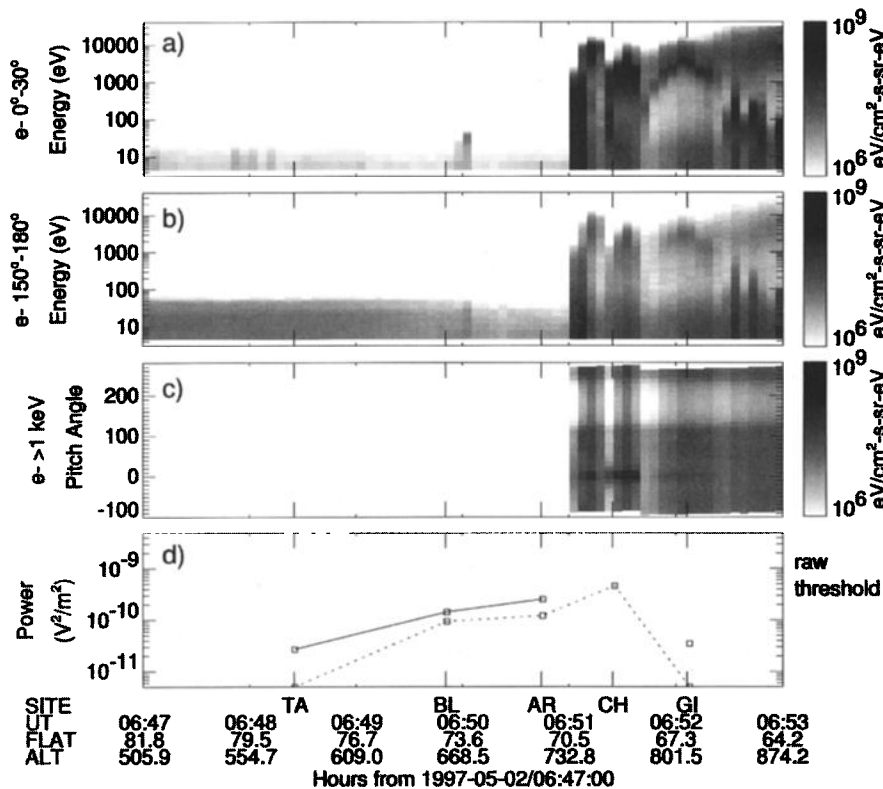


**Figure 10.** Data from electrostatic analyzers aboard FAST during orbit 2745 showing electron energy flux versus energy for (a)  $0^\circ$ – $30^\circ$  and (b)  $150^\circ$ – $180^\circ$  pitch angle ranges. (c) Electron energy flux versus pitch angle are shown for energies  $>1$  keV. (d) Integrated PSFR power averaged for 4 min when FAST crosses the polar cap boundary. The altitude of the spacecraft and the invariant latitude of its footprint are indicated below Figure 10d.

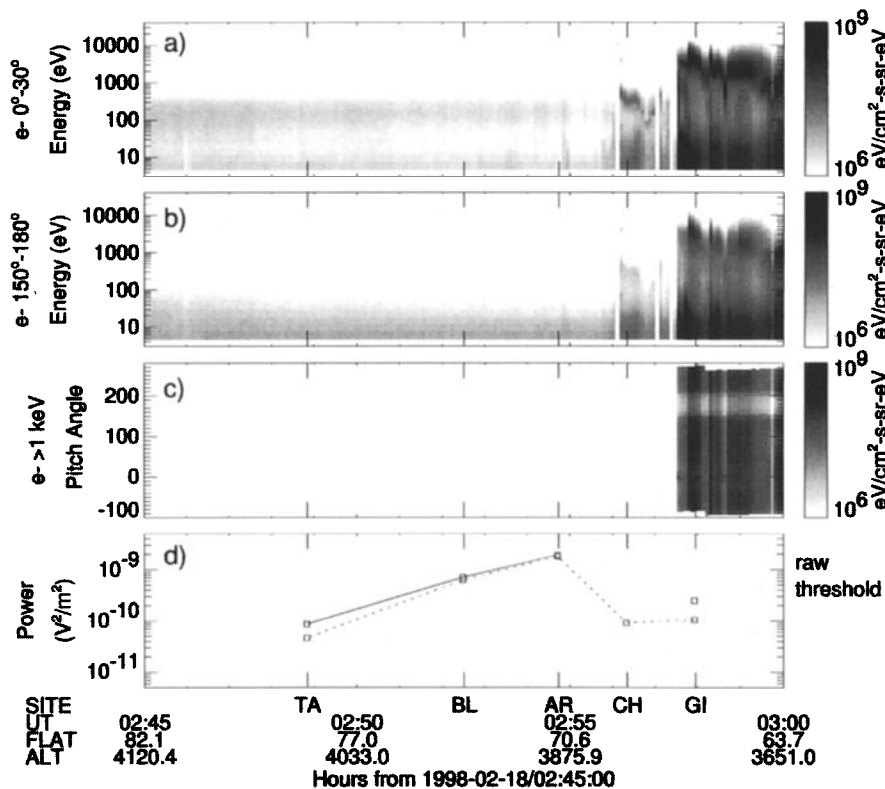


**Figure 11.** Data from electrostatic analyzers aboard FAST during orbit 5903 showing electron energy flux versus energy for (a)  $0^{\circ}$ – $30^{\circ}$  and (b)  $150^{\circ}$ – $180^{\circ}$  pitch angle ranges. (c) Electron energy flux versus pitch angle are shown for energies  $>1$  keV. (d) Integrated PSFR power averaged for 4 min when FAST crosses the polar cap boundary. The altitude of the spacecraft and the invariant latitude of its footprint are indicated below Figure 11d.

tometer data (upper dashed line in Figure 6g) is within  $1^{\circ}$  latitude.

Figure 10d suggests that during the conjunction the intensity of the emissions is greatest at Churchill ( $69^{\circ}$ ), which lies at the poleward boundary of the auroral precipitation to within the resolution of the ground-based receivers. An inverted-V structure extending to nearly 10 keV, shown in Figure 10a, is centered near  $69^{\circ}$  latitude implying that energetic electrons are present at the latitude of the emissions. Also present on field lines near the location of the most intense auroral roar are upgoing loss cone ( $180^{\circ}$ ) and downgoing beam ( $0^{\circ}$ ) distributions (Figure 10c) which are possible sources of a plasma instability which may generate auroral roar [Weatherwax *et al.*, 1995; Yoon *et al.*, 1996].

#### 4.2. February 17, 1998

Figure 9 shows the footprint of FAST during its orbit (5903) on February 17, 1998. In contrast to the previous orbit this orbit was an apogee pass of the Northern Hemisphere, and the altitude of the spacecraft was  $\sim 4000$ – $3500$  km. The footprint of FAST passes near several of the ground stations during the period  $\sim 0249$ – $0257$  UT ( $\sim 1900$ – $2000$  MLT).

The footprint of FAST passes the polar cap boundary at  $\sim 0257:30$  UT ( $\sim 67^{\circ}$ ) in Figure 11, although some low-energy ( $\sim 1$  keV) precipitating electrons are seen

shortly before at 0257:10 UT ( $\sim 69^{\circ}$ ). The polar cap boundary as seen by FAST agrees to within  $\sim 1.5^{\circ}$  of the poleward electrojet boundary inferred from the magnetometers at this time (Figure 7). The agreement is reasonable considering the spacing of the magnetometers.

Figure 11d suggests that the intensity of the emissions peaks near Arviat,  $\sim 3^{\circ}$  poleward of the most northern auroral arc intersected by FAST. The low-energy ( $\leq 1$  keV) precipitating electrons located farther poleward of this arc are probably not energetic enough to be the source of auroral roar emissions; however, they may be effective in screening emissions. An inverted-V structure shown in Figure 11a is located at the latitude of Gillam as well as upgoing loss cone ( $180^{\circ}$ ) and trapped ( $40^{\circ}$ – $130^{\circ}$ ) electron populations. In five other FAST overpasses (not shown), downgoing beams, upgoing loss cones, and trapped electron populations are present implying that energetic electrons capable of generating auroral roar are present near or equatorward of the emissions.

## 5. Discussion and Summary

Hughes and LaBelle [1998] surveyed auroral roar at various latitudes to show that the peak occurrence rate of  $2f_{ce}$  emissions is surprisingly near the statistical poleward edge of the auroral zone ( $75^{\circ}$ – $76^{\circ}$  invariant) rather

than the middle of the auroral zone. The five events described in section 4 are the first auroral roar emissions studied in detail by observing the emissions simultaneously with receivers spread over a range of latitudes that sample the polar cap and auroral zone and by comparing these observations with ground magnetometer and satellite data. The work presented in this study suggests why auroral roar peaks in occurrence at the poleward edge of the auroral zone as suggested by *Hughes and LaBelle* [1998].

In four of the 5 days studied, the peak intensity of auroral roar emissions is located at or poleward of the poleward electrojet boundary inferred from the magnetometers, often by many degrees or many hundreds of kilometers. During the October 3 event (Figure 3) the peak intensity remained up to  $9^\circ$  poleward of the electrojet boundary for all but a few brief periods. The same behavior occurs during the October 4 event (Figure 4) except for brief periods when the electrojet boundary is moving rapidly (e.g., 0045 UT). Again, during the November 5 event (Figure 5) the intensity peaks poleward of the electrojet boundary by up to  $7^\circ$ , except for a few brief moments. During the February 17 event (Figure 7) the location of the peak intensity is again nearly always poleward of the electrojet boundary by up to  $6^\circ$ , except for one brief burst of auroral roar detected at Gillam at 0405 UT and after  $\sim$ 0600 UT when the latitude of the electrojet boundary changes rapidly.

The May 2 event (Figure 6) is strikingly in contrast to the other 4 days. The intensity most of the time peaks many degrees, often up to  $10^\circ$ , equatorward of the poleward electrojet boundary, closer to the middle of the auroral zone, and for a short time (0428 UT) equatorward of the equatorward electrojet boundary. This unexpected result could be explained by the presence of double or multiple auroral arcs. Perhaps emissions can penetrate to the ground between the poleward and equatorward emission regions. There is evidence during some of this period ( $\sim$ 0500–0645 UT) for double electrojet structures, inverted-V type structures with latitudinal scale sizes of  $\sim$ 100 km, in the magnetometer and meridian scanning photometer data. Furthermore, the auroral roar recorded between the two substorms from  $\sim$ 0425 to 0700 UT sometimes has a very different character at adjacent sites or is detected only at a single site, indicating that several sources are involved during this period. However, the strong auroral roar recorded after 0230 UT which occurs at all five sites and peaks  $\sim$  $7^\circ$  equatorward of the poleward electrojet boundary, is clearly generated at a single source.

It is not clear whether all of the emissions observed within the auroral zone can be explained by double electrojet structures. Another possibility is that auroral roar sometimes occurs when the aurora has severe longitudinal structure, so that the emission is poleward of its causative arc but equatorward of the average boundary defined by the magnetometer data. During periods of high activity, such as substorms, current structures can become wrapped up or kinked and located at dif-

ferent latitudes on closely spaced longitudes. The magnetometer array may not resolve such kinks if they are  $< \sim 10^\circ$  wide. This explanation is consistent with the observations of periods when the electrojet boundary is moving rapidly poleward, that is, during a substorm, and the peak intensity of emissions appears to lag, as in the November 5 event at 0050 UT when the electrojet boundary moves from  $69.9^\circ$  to  $76.2^\circ$  and the peak intensity remains fixed near Arviat at  $\sim 71^\circ$ . This idea does not apply to the May 2 event, where the peak intensity of the emissions is consistently equatorward of the poleward electrojet boundary for many hours.

*Kellogg and Monson* [1979] observed that auroral roar emissions were screened when auroral arcs moved directly overhead. The explanation given is that the electron precipitation responsible for the auroral arcs, and most likely for the auroral roar emissions, ionizes the lower layers of the ionosphere (*E* and *D*), raising the plasma frequency ( $f_{pe}$ ) cutoff in these regions above the frequency of the emissions, preventing them from propagating to the ground. *Kellogg and Monson* [1984] speculate that no auroral roar emissions were detected at Cleary, Alaska ( $\sim 59^\circ$   $\Lambda$ ) because diffuse aurora was always present, screening them from the source region. Further evidence of screening was given by *Weatherwax et al.* [1995] using a meridian scanning photometer colocated with a PSFR and also given by *Shepherd et al.* [1998a] using electron density profiles from the incoherent scatter radar at the Sondrestrom Radar Facility.

Evidence of screening can be seen in many of the examples presented in this study. For example, during the October 3 event from 0200 to 0300 UT (Figure 3), auroral roar is detected very strongly at Arviat and Baker Lake, falls off in intensity at Taloyoak, occurs only intermittently at Churchill, the location of the electrojet boundary, and is not detected at Gillam, which is inside the auroral zone. Between 0300 and 0310 UT, emissions are briefly detected at Gillam only after the poleward boundary of the electrojet moves equatorward of the latitude at this station. These data suggest that the auroral roar occur continuously, but the stations at which they are observed are controlled by the screening ionization generated by auroral precipitation.

It is curious that in some cases the most intense auroral roar emission are up to  $7^\circ$  poleward of the auroral zone, inside the polar cap where there are no apparent sources of free energy to generate these waves. In these cases, auroral roar emissions must propagate poleward from lower latitudes to explain the observations. If the wave intensity falls off as the distance from the source increases, one would expect the emissions to peak at the station in the polar cap which is nearest the source, not at a station which is even farther poleward. One possible explanation is that the emissions are not generated isotropically and preferentially propagate at larger angles to the background magnetic field.

Another possibility is suggested by Figure 11a, which shows a relatively narrow ( $\sim 2^\circ$ ) region of low-energy ( $\sim 1$  keV) electron precipitation poleward of the most

northern auroral arc. These low-energy precipitating electrons do not produce significant conductivity necessary to significantly affect ionospheric currents, nor are they energetic enough to generate auroral roar. However, they may be energetic enough to produce ionization capable of partially screening emissions. Waves generated at the lower latitude inverted-V near Gillam (67°) traveling along paths to Churchill (69°) pass through this somewhat tenuous layer and are partially absorbed, while those directed to higher latitudes at Arviat (71°) pass over this layer and are unaffected. The result is an apparent peak of emission intensity at the higher latitude of Arviat, 5° poleward of the auroral zone, and weaker emissions at Churchill, 3° poleward.

Partial screening of auroral emissions suggests another possible explanation for why emissions are sometimes detected inside the auroral oval, which is that they may not be entirely screened. During the three periods when auroral roar is detected at Gillam during the May 02, 1997, event (0230, 0415, and 0645 UT), the ground-level magnetic field fluctuations due to the electrojet currents are <150 nT, weaker than periods when emission are not seen at Gillam. It is possible that the weaker precipitation-induced ionization associated with this weaker electrojet allows emissions to propagate where they would normally be completely reabsorbed or reflected by the plasma.

In all of the 5 days studied, periods exist during which the peak intensity of auroral roar emissions appears to track with the poleward edge of the electrojet. This effect probably results from a combination of the auroral roar source region moving as the oval expands or contracts and the emissions being screened from sites equatorward of the most poleward region of precipitation. It is also possible that ionospheric cavities, such as those described by Doe *et al.* [1993], which tend to occur poleward of the statistical auroral oval, play a role in auroral roar generation and thus explain why the emissions follow the movement of the poleward boundary [Shepherd *et al.*, 1998a].

The observations during the five study days presented in this paper are consistent with auroral roar being generated by the precipitating electrons at the latitudes of inverted-V structures. Electrons capable of generating auroral roar are observed at altitudes above the probable source region by the FAST satellite in all eight conjunctions studied. The emissions are free to propagate into the tenuous plasma of the polar cap and are reflected and/or reabsorbed by the precipitation-induced ionospheric layers in the auroral zone. The resulting intensity of emissions detected on the ground appears to peak at or near the latitude of the most poleward inverted-V structure or, on occasions, poleward of that location. Multiple inverted-V structures and dynamic precipitation boundaries can produce conditions such that auroral emissions are seen and peak inside the auroral zone.

It is unknown whether auroral roar is generated over a wide range of latitudes spanning the auroral zone and

only emissions from a narrow region near the poleward edge propagate to the ground or whether emissions are only generated in a narrow region near the poleward edge at the most poleward inverted-V structure. A phased antenna array is being deployed at the Sondrestrom Radar Facility near Kangerlussuaq, Greenland, this year by Dartmouth College researchers. The direction finding capabilities of this system will allow the source location to be better determined.

**Acknowledgments.** The authors thank M. L. Trimpi for designing the Dartmouth College radio receivers and R. Brittain for software contributions. David St. Jacques, the Churchill Northern Studies Centre, Ralph King, the Canadian Geological Survey, and Rodger Mannilaq maintained the radio receivers at remote sites. E. J. Lund, W. Peria, and C. C. Chaston provided assistance with analyzing the FAST data, and H. al Nashi prepared the CANOPUS border position estimates. This research was supported by National Science Foundation grant ATM-9713119 to Dartmouth College. The CANOPUS array was constructed and is operated by the Canadian Space Agency. The work at the University of Alberta was supported by the Natural Sciences and Engineering Research Council of Canada under grant OGP5420.

Hiroshi Matsumoto thanks N. Sato and another referee for their assistance in evaluating this paper.

## References

- Baker, K. B., and S. Wing, A new coordinate system for conjugate studies at high latitudes, *J. Geophys. Res.*, *94*, 9139, 1989.
- Carlson, C. W., R. F. Pfaff, and J. G. Watzin, The Fast Auroral SnapshoT (FAST) mission, *Geophys. Res. Lett.*, *25*, 2013, 1998.
- Doe, R. A., M. Mendillo, J. F. Vickrey, L. J. Zanetti, and R. W. Eastes, Observations of nightside auroral cavities, *J. Geophys. Res.*, *98*, 293, 1993.
- Gustafsson, G., N. E. Papitashvili, and V. O. Papitashvili, A revised corrected geomagnetic coordinate system for epochs 1985 and 1990, *J. Atmos. Terr. Phys.*, *54*, 1609, 1992.
- Hughes, J. M., and J. LaBelle, The latitude dependence of auroral roar, *J. Geophys. Res.*, *103*, 14,911, 1998.
- International Association of Geomagnetism and Aeronomy Division I Working Group 1, International geomagnetic reference field: Revision 1985, *J. Geomagn. Geoelectr.*, *37*, 1157, 1985.
- Kellogg, P. J., and S. J. Monson, Radio emissions from the aurora, *Geophys. Res. Lett.*, *6*, 297, 1979.
- Kellogg, P. J., and S. J. Monson, Further studies of auroral roar, *Radio Sci.*, *19*, 551, 1984.
- Kellogg, P. J., S. J. Monson, and B. A. Whalen, Rocket observation of high frequency waves over a strong aurora, *Geophys. Res. Lett.*, *5*, 47, 1978.
- Kisabeth, J. L., The dynamical development of the polar electrojets, Ph.D. thesis, Univ. of Alberta, Edmonton, Alberta, Canada, 1972.
- LaBelle, J., A. T. Weatherwax, M. L. Trimpi, R. Brittain, R. D. Hunsucker, and J. V. Olson, The spectrum of LF/MF/HF radio noise at ground level during substorms, *Geophys. Res. Lett.*, *21*, 2749, 1994.
- LaBelle, J., M. L. Trimpi, R. Brittain, and A. T. Weatherwax, Fine structure of auroal roar emissions, *J. Geophys. Res.*, *100*, 21,953, 1995.
- Rostoker, G., Nowcasting of space weather using the CANOPUS magnetometer array, *Phys. in Canada, Sep./Oct.*, 277, 1998.

- Rostoker, G., J. C. Samson, F. Creutzberg, T. J. Hughes, D. R. McDiarmid, A. G. McNamara, A. V. Jones, D. D. Wallis, and L. L. Cogger, CANOPUS – A ground-based instrument array for remote sensing the high latitude ionosphere during the ISTP/GGS program, *Space Sci. Rev.*, *71*, 743, 1995.
- Shepherd, S. G., J. LaBelle, and M. L. Trimpi, The polarization of auroral radio emissions, *Geophys. Res. Lett.*, *24*, 3161, 1997.
- Shepherd, S. G., J. LaBelle, R. A. Doe, M. McCreedy, and A. T. Weatherwax, Ionospheric structure and the generation of auroral roar, *J. Geophys. Res.*, *103*, 29,253, 1998a.
- Shepherd, S. G., J. LaBelle, and M. L. Trimpi, Further investigation of auroral roar fine structure, *J. Geophys. Res.*, *103*, 2219, 1998b.
- Weatherwax, A. T., J. LaBelle, M. L. Trimpi, and R. Brittain, Ground-based observations of radio emissions near  $2f_{ce}$  and  $3f_{ce}$  in the auroral zone, *Geophys. Res. Lett.*, *20*, 1447, 1993.
- Weatherwax, A. T., J. LaBelle, M. L. Trimpi, R. A. Treumann, J. Minow, and C. Deehr, Statistical and case studies of radio emissions observed near  $2f_{ce}$  and  $3f_{ce}$  in the auroral zone, *J. Geophys. Res.*, *100*, 7745, 1995.
- Yoon, P. H., A. T. Weatherwax, T. J. Rosenberg, and J. LaBelle, Lower ionospheric cyclotron maser theory: A possible source of  $2f_{ce}$  and  $3f_{ce}$  auroral radio emissions, *J. Geophys. Res.*, *101*, 27,015, 1996.
- 
- C. W. Carlson, Space Sciences Laboratory, University of California, Berkeley, Berkeley, CA 94720. (cwc@ssl.berkeley.edu)
- J. LaBelle, Department of Physics and Astronomy, Dartmouth College, Wilder Hall, Hinmann Box 6127, Hanover, NH 03755. (jlabelle@einstein.dartmouth.edu)
- G. Rostoker, Department of Physics, University of Alberta, Edmonton, AB, Canada, T6G 2J1 (rostoker@space.ualberta.ca)
- S. G. Shepherd, Applied Physics Laboratory, Johns Hopkins University, 11100 Johns Hopkins Road, Laurel, MD 20723. (simon.shepherd@jhuapl.edu)

(Received February 25, 1999; revised April 30, 1999; accepted April 30, 1999.)